

H_I in XMD Galaxies III. GMRT observations of BCG HS 0822+3542

Jayaram N. Chengalur^{1,2*} S.A. Pustilnik^{3†} J.-M. Martin^{4‡} A.Y. Kniazev^{5,3§}

¹ ATNF/CSIRO, P. O. Box 76, Epping NSW 1710, Australia

² NCRA (TIFR), Pune University Campus, Postbag 3, Ganeshkhind, Pune 411007, India

³ Special Astrophysical Observatory RAS, Nizhnij Arkhyz, Karachai-Circassia, 369167 Russia

⁴ Observatoire de Paris, 5, place J. Janssen, 92195 Meudon Cedex, France

⁵ South African Astronomical Observatory, Cape Town, South Africa

Accepted 2006 . Received 2006

ABSTRACT

We present the results of Giant Metrewave Radio Telescope H_I 21-cm line observations of the eXtremely Metal Deficient (XMD) blue compact galaxy (BCG) HS 0822+3542. HS 0822+3542 is the smallest known XMD galaxy; from HST imaging it has been suggested that it actually consists of two still smaller (~ 100 pc sized) ultra-compact dwarfs that are in the process of merging. The brighter of these two putative ultra compact dwarfs has an ocular appearance, similar to that seen in galaxies that have suffered a penetrating encounter with a smaller companion. From our H_I imaging we find that the gas distribution and kinematics in this object are similar to that of other low mass galaxies, albeit with some evidence for tidal disturbance. On the other hand, the H_I emission has an angular size ~ 25 times larger than that of the putative ultra-compact dwarfs. The optical emission is also offset from the centre of the H_I emission. HS 0822+3542 is located in the nearby Lynx-Cancer void, but has a nearby companion LSB dwarf galaxy SAO 0822+3545. In light of all this we also consider a scenario where the optical emission from HS 0822+3542 comes not from two merging ultra-compact dwarfs but from multiple star forming regions in a tidally disturbed galaxy. In this model, the ocular appearance of the brighter star forming region could be the result of triggered star formation.

Key words: galaxies: ISM – galaxies: star formation – galaxies: low surface brightness – galaxies: interaction – galaxies: kinematics and dynamics – ISM: H_I – galaxies: individual (HS 0822+3542, SAO 0822+3545)

1 INTRODUCTION

The metallicity of the ISM of external galaxies is often quantified in terms of the oxygen abundance, which, in turn, is generally expressed in terms of the quantity $12 + \log(O/H)$. A very small fraction of gas-rich dwarfs have $12 + \log(O/H) \lesssim 7.65$, i.e. an oxygen abundance of less than $\sim 1/10$ solar. These dwarfs, (the majority of which are also members of Blue Compact Galaxy (BCG) class), are termed eXtremely Metal Deficient (XMD) galaxies (see Kunth & Östlin (2000) for a review). Low oxygen abundances are naturally expected for galaxies that have only recently experienced their first episode of star formation. For example, metallicities of

$\lesssim 1/10$ solar are typical of high redshift Damped Lyman- α systems (e.g., Pettini et al. 1997), which are widely regarded as proto-galactic objects. It is now well established that the majority of (but not all) well studied XMD galaxies have a substantial mass fraction of their stellar mass in old stars (see e.g. a brief review in Pustilnik & Martin 2006) and are hence not forming stars for the first time. Nonetheless, their very low ISM metallicity still makes them the best local analogs of young galaxies at high redshift. Detailed studies of XMD galaxies should hence give insight into galaxy evolution in the early universe.

While the *fraction* of XMD BCGs in the Local Universe is very small ($\lesssim 2\%$ of all known BCGs, e.g., Pustilnik et al. 2005), the *number* of known XMD galaxies has seen a dramatic increase in the recent past, via new large surveys for emission line galaxies (e.g. HSS, KISS and SDSS), and ~ 60 such galaxies are now known. However, detailed optical and

* chengalur@ncra.tifr.res.in

† sap@sao.ru

‡ jean-michel.martin@obspm.fr

§ aknizhev@sao.ac.za

Table 1. Parameters of the GMRT observations

Parameters	Value
RA (2000)	$08^h 25^m 55.4^s$
Declination (2000)	$35^\circ 32' 32''$
Date of observations	18 & 30 June 2001
Time on source	7 hrs
Total bandwidth	2.0 MHz
Number of channels	128
Channel separation	3.3 km sec^{-1}
FWHM of synthesized beam	$42'' \times 37'', 27'' \times 23'', 17'' \times 15'', 4'' \times 3''$
RMS (at 6.6 km s^{-1} resolution)	1.3 mJy, 1.1 mJy 1.0 mJy, 0.7 mJy

radio observations are currently available only for a very small fraction of them. As less evolved galaxies, XMDs are expected to be very gas-rich, and indeed for some objects (e.g., SBS 0335–052; Pustilnik et al. 2001, 2004), the gas makes up $\sim 99\%$ of the total baryonic mass. $\text{H}\alpha$ observations are hence critical in understanding the nature of these rare galaxies. For some of XMD BCGs from the Second Byurakan Survey (SBS) the integrated $\text{H}\alpha$ parameters are available in Thuan et al. (1999). More recently, Pustilnik & Martin (2006) (Paper I) conducted single dish $\text{H}\alpha$ observations for 22 XMD galaxies. Follow-up aperture synthesis $\text{H}\alpha$ observations of these galaxies are now in progress (e.g. BCG SBS 1129+576 Ekta, et al. (2006), (Paper II)).

In this paper we present Giant Metrewave Radio Telescope (GMRT) $\text{H}\alpha$ 21cm observations of one of the nearest known XMD BCGs, HS 0822+3542 ($12 + \log(\text{O/H}) = 7.35$; Kniazev et al. 2000). Pustilnik et al. (2003) found that this galaxy has a companion at a projected separation of $3.8'$ (i.e. ~ 11.4 kpc at the distance to the pair¹) – the Low Surface Brightness (LSB) dwarf galaxy SAO 0822+3545. The separation between HS 0822+3542 and SAO 0822+3545 is much smaller than that of the primary beam of the GMRT antennas, and our observations are sensitive to $\text{H}\alpha$ emission from both of them. In Sec. 2 we describe the GMRT observations and data reduction. Results are presented in Sec. 3 and discussed in Section 4.

2 OBSERVATIONS AND REDUCTION

GMRT (Swarup et al. 1991) observations of HS 0822+3542 were conducted on 18th and 30th June, 2001, when the telescope was in its commissioning phase. The setup for the observations is given in Table 1. Absolute flux calibration and bandpass calibration were done using scans on the standard calibrators 3C48 and 3C286, one of which was observed at the start and end of each observing run. Phase calibration was done using the VLA calibrator source 0741+312 which was observed once every 45 minutes. The data were reduced using standard tasks in classic AIPS. For each run, bad visibility points were edited out, after which the data were calibrated. Calibrated data for both runs were combined using

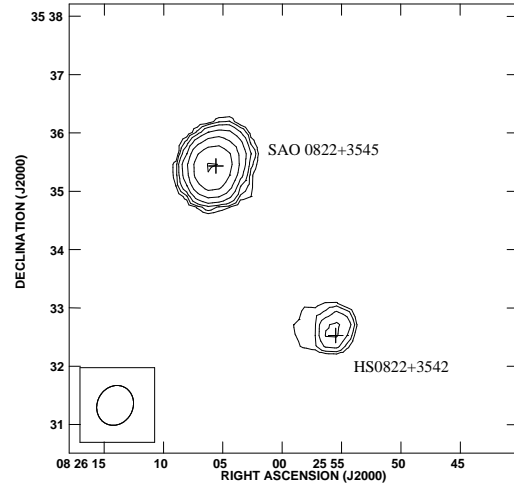


Figure 1. GMRT $42'' \times 37''$ resolution integrated $\text{H}\alpha$ emission map from HS 0822+3542 and SAO 0822+3545. The contour levels are at 2.5 (i.e. $\sim 4\sigma$), $4.4, 7.7, 13.3, 21.3$, and 40.2×10^{19} atoms cm^{-2} . The crosses mark the centres of the optical galaxies.

DBCON. The GMRT does not do online Doppler tracking – the differential Doppler shift between the two runs was hence corrected for using the AIPS task CVEL before combining the two observing runs. The GMRT has a hybrid configuration and a single GMRT observation can be used to make maps at a range of angular scales. Data cubes were therefore made at resolutions ranging from $\sim 40''$ to $\sim 3''$. Continuum was subtracted using the AIPS task IMLIN, and the data cubes were cleaned using APCLN. Finally moment images were made using the AIPS task MOMNT.

The $\text{H}\alpha$ emission from the galaxy pair spans 24 channels of the spectral cube. A continuum image was made using the average of remaining line free channels. The only detected emission was from a faint (~ 7 mJy) source at $08^h 25^m 59.3^s + 35^\circ 31' 12''$, i.e. $1.2'$ southeast of the $\text{H}\alpha$ emission seen from HS 0822+3542. Given that the location of the continuum emission is outside the $\text{H}\alpha$ disk, it appears likely that it is a background source, not associated HS 0822+3542. This is consistent with the NED entries for this position (i.e. a FIRST source with $f_\nu(1.4 \text{ GHz}) \sim 4$ mJy, and a 2MASS galaxy).

3 RESULTS

3.1 Morphology and density distribution

The integrated $\text{H}\alpha$ emission from HS 0822+3542 and SAO 0822+3545 at an angular resolution of $42'' \times 37''$ is shown in Fig. 1. Synthetic single dish spectra are shown in Fig. 2. There is a hint of tidal distortion seen in the lowest contour of HS 0822+3542. The parameters derived from the synthetic profiles are summarised in Tab. 2. The bulk of the $\text{H}\alpha$ flux from this pair comes from the companion LSB galaxy SAO 0822+3545. If the emission from the two galaxies is

¹ We assume a distance of 11 Mpc. At this distance $1''$ corresponds to a linear separation of ~ 53 pc.

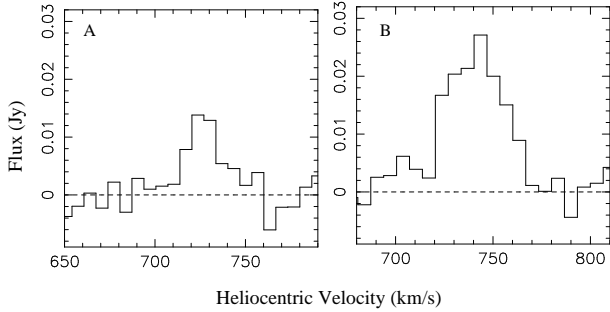


Figure 2. Synthetic single dish HI profiles for HS 0822+3542 (panel A) and SAO 0822+3545 (panel B). The channel separation is 6.6 km s^{-1} .

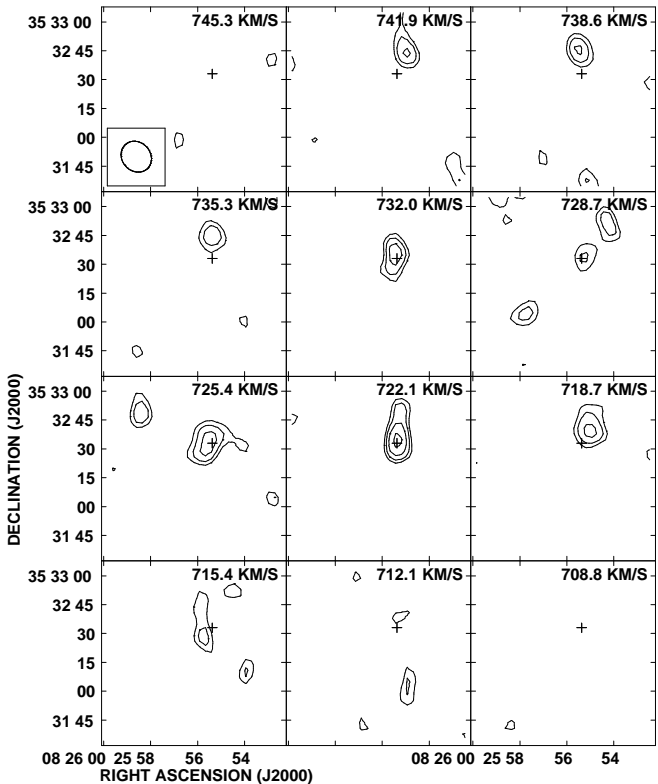


Figure 3. Channel maps of the HI emission from HS 0822+3542 at a resolution of $17'' \times 15''$. The contours are at 3.4, 4.4, 5.6 and 7.2 mJy/Bm. The cross marks the position of the optical galaxy

added together, the resulting profile (not shown) is a reasonable match to that obtained at the NRT by Kniazev et al. (2000), where the beam covered both galaxies. As expected, the total flux obtained by the NRT is somewhat lower than that obtained by the GMRT. This is because the brighter galaxy in the pair was close to the half-power point of the NRT beam.

In Fig. 3 we show channel maps of the emission from HS 0822+3542 at a resolution of $17'' \times 15''$. The signal-to-noise ratio is marginal, but it can still be seen that the

centroid of the emission shifts from north to south as one moves towards lower heliocentric velocities.

In Fig. 4 we show overlays of the SDSS *r*-band (Abazajian et al. 2005) optical emission and the HI emission from HS 0822+3542 and SAO 0822+3545. The HI extension to the north-east of HS 0822+3545 seen in Fig. 1 can also be seen in Fig. 4[A] & [B], although at these resolutions the emission does not connect to the main body. This could be a consequence of both the marginal signal-to-noise ratio as well as the lower sensitivity to diffuse emission in these maps. One can also see a tidal tail like extension from the northern end of HS 0822+3542 (most clearly in panel [B]). The HI emission (apart from these features) is fairly symmetric about its peak. The HI emission is unusually extended compared to the optical emission, but even more unusual is the large offset between the optical emission and the centre of the HI emission. While the HI distribution seems in general uncorrelated with the optical emission, one can see in Fig. 4[C] a kink in the HI contours aligned with the diffuse plume of optical emission extending to the north-west.

The velocity fields for SAO 0822+3545 and HS 0822+3542 (as derived from the first moment of the $27'' \times 23''$ resolution data cube) are shown in Fig. 5. We note that the spatial resolution is marginal (particularly so for HS 0822+3542); the inferences we make below should hence be regarded as tentative.

For SAO 0822+3545, the velocity field appears regular, with an indication of a warp in the outer parts, i.e. starting from the edge of the optical disk. From an inspection of the velocity field, one can crudely estimate the inclination corrected (where the inclination is computed from the optical image, see Table 2) rotation velocity to be $\sim 14 \text{ km s}^{-1}$. For HS 0822+3542, a north-south velocity gradient, consistent with that seen in the channel maps is seen in the velocity field. If this is indicative of rotation, the implied rotational velocity is extremely small, viz. $\sim 4 \text{ km s}^{-1}$ (i.e. smaller than the velocity dispersion, see below).

The velocity dispersion, σ , in galaxies of comparable HI mass to SAO 0822+3545 and HS 0822+3542 is $\sigma \sim 7-9 \text{ km s}^{-1}$ (see, e.g., Begum et al. 2006), i.e., comparable to the peak rotation speed in the galaxies. Clearly, both rotation as well as random velocities are important in supporting the HI disk against collapse. Determining the dynamical mass from the observed velocity field hence requires correction for the support provided by the pressure gradient in the disk. Computing this requires one to have a good estimate of the density gradient across the disk (see, e.g., Begum et al. (2003); Begum & Chengalur 2004). The modest signal-to-noise ratio and spatial resolution of our data would result in substantial systematic uncertainties, were we to try this approach. We instead compute an indicative dynamical mass following Staveley-Smith et al. (1992). In detail, we assume that $W_{50} \sim 2(V_{\text{rot}} \sin(i) + 1.18\sigma)$ and $M_{\text{dyn}} = 3.3 \times 10^4 a_H D (V_{\text{rot}}^2 + 3\sigma^2)$, where D is the distance in Mpc and a_H is the diameter in arcmin. For SAO 0822+3545 taking $a_H \sim 1.5$, $\sigma \sim 7$, and the inclination listed in Tab 2, gives $V_{\text{rot}} \sim 10 \text{ km s}^{-1}$ and $M_{\text{dyn}} \sim 1.4 \times 10^8 M_{\odot}$. Assuming a similar velocity dispersion for HS 0822+3542 and an angular diameter of $\sim 0.75'$ gives $V_{\text{rot}} \sim 3 \text{ km s}^{-1}$ and $M_{\text{dyn}} \sim 4 \times 10^7 M_{\odot}$. The low ratio of

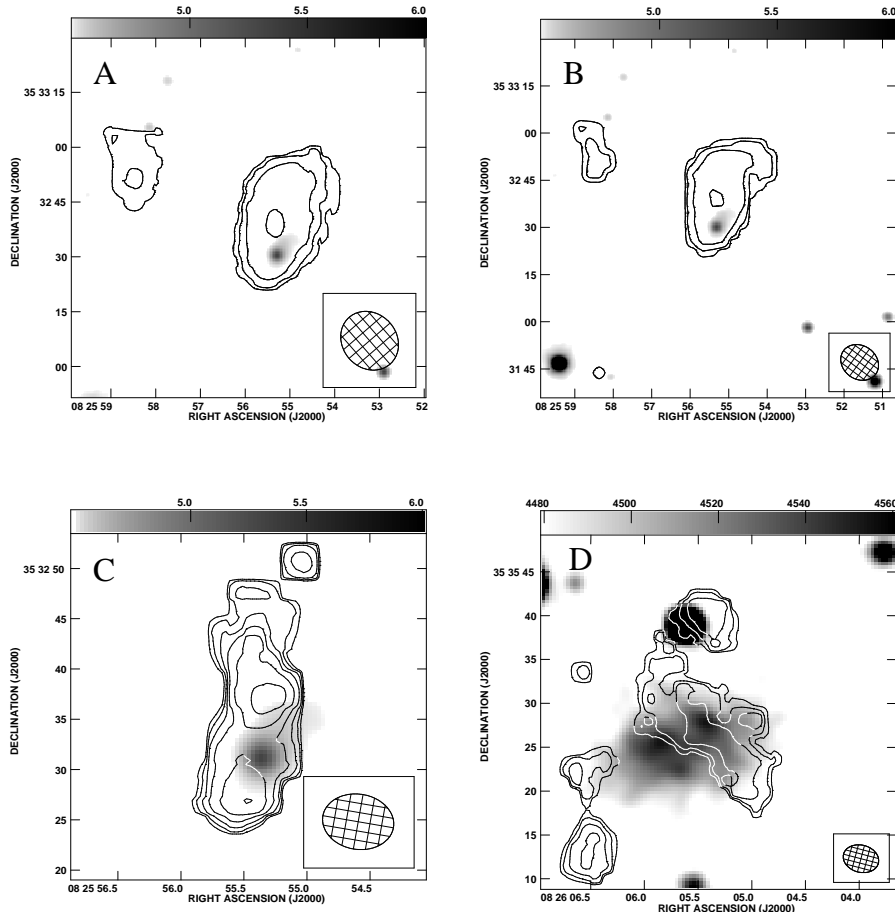


Figure 4. Overlay of the SDSS r -band optical emission (grey scales) on the integrated $\text{H}\alpha$ emission (contours) from HS 0822+3542 and SAO 0822+3545. [A] HS 0822+3545, resolution $17'' \times 15''$. The contours are at $0.52, 1.2, 2.6$ and 5.7×10^{20} atoms cm^{-2} . [B] HS 0822+3545, resolution $13'' \times 11''$. The contours are at $0.23, 0.75, 2.4$ and 7.8×10^{20} atoms cm^{-2} . [C] HS 0822+3545, resolution $7'' \times 5.5''$. The contours are at $2.3, 3.3, 4.6, 6.6, 9.3$ and 13.2×10^{20} atoms cm^{-2} . [D] SAO 0822+3545, resolution $4'' \times 3.1''$. The contours are at $0.74, 1.3, 2.2$ and 3.7×10^{21} atoms cm^{-2} . Note that the optical emission seen coincident with the northern most $\text{H}\alpha$ emission is an unrelated foreground star.

V_{rot}/σ in HS 0822+3542 is typical of very low mass dwarf galaxies (see eg. Begum et al. 2006).

4 DISCUSSION

The main $\text{H}\alpha$ and optical parameters of HS 0822+3542 and SAO 0822+3545 are summarised in Tab. 2. Using deconvolved Nordic Optical Telescope images, Pustilnik et al. (2003) found that the bright knot of optical emission in HS 0822+3542 consists of two components. Based on HST images, Corbin et al. (2005) state that these two components have a surface brightness that is ~ 100 times larger than that of the diffuse emission extending to the north west. The brighter of these two components (component “A” in the terminology of Corbin et al. (2005); see their Fig 1) has an ocular morphology, with a central blue star forming region surrounded by a ring of redder stars. The fainter component (component “B”) is ~ 5 times less luminous and

more irregular in appearance. Morphologies similar to that of component “A” are seen in galaxies where there has been a penetrating encounter with a smaller companion (e.g., the Cartwheel galaxy). Based on this, Corbin et al. (2005) suggest that HS 0822+3542 is actually a system of two merging ultra-compact dwarfs, and that it represents a dwarf galaxy in the process of formation.

Our $\text{H}\alpha$ observations show that the gas in this system appears to have settled into a disk with fairly regular kinematics. We note again however, that this may be a consequence of our marginal angular resolution. In any case, a regular $\text{H}\alpha$ disk may be consistent with the merger scenario – recent numerical simulations show that in gas-rich mergers, the gas quickly settles into a disk (Springel & Hernquist 2005). On the observational front, there are cases of merging galaxies where a large fraction of the gas does seem to have settled into a disk (e.g., IC 2554, Koribalski et al. (2003); NGC 3310 Kregel & Sancisi 2001). $\text{H}\alpha$ observations of the Cartwheel galaxy itself (Higdon 1996) show that the gas is

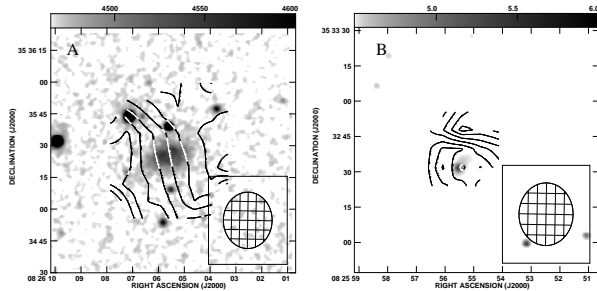


Figure 5. [A] The velocity field of SAO 0822+3545 as derived from the $27'' \times 23''$ resolution data cube. The velocity contours are at 732, 735, 738, 741, 744, 747, 750, 753 and 756 km s^{-1} (heliocentric). The grey scale is the SDSS r -band image. [B] The velocity field of HS 0822+3542 as derived from the $27'' \times 23''$ resolution data cube. The velocity contours are at 722, 723, 724, 725, 726, 727 and 728 km s^{-1} (heliocentric). The grey scale is the SDSS r -band image.

Table 2. Main parameters of the studied galaxies

Parameter	HS 0822+3542	SAO 0822+3545
R.A.(J2000.0)(opt)	08 25 55.47	08 26 05.59
DEC.(J2000.0)(opt)	+35 32 32.9	+35 35 25.7
B_{tot}	$17.92 \pm 0.05^{(1)}$	$17.56 \pm 0.03^{(3)}$
$V_{\text{hel}}(\text{HI})(\text{km s}^{-1})$	$726.6 \pm 2^{(2)}$	$740.7 \pm 1.3^{(2)}$
Dist ⁽³⁾ (Mpc)	11.0	11.0
M_B^0 ⁽⁴⁾	-12.49	-12.85
Opt. size ('') ⁽⁵⁾	$14.8 \times 7.4^{(1)}$	$28.2 \times 15.5^{(3)}$
Opt. size (kpc)	0.79×0.39	$1.50 \times 0.83^{(3)}$
Inclination (deg) ⁽⁶⁾	62	59
$12 + \log(\text{O/H})$	$7.44^{(3)}$	—
HI int.flux ⁽⁷⁾	$0.27 \pm 0.06^{(2)}$	$0.83 \pm 0.08^{(2)}$
W_{50} (km s^{-1})	$21.7 \pm 4^{(2)}$	$35.5 \pm 3^{(2)}$
V_{rot} (HI) (km s^{-1})	$\leq 5^{(2)}$	$14^{(2)}$
$M(\text{HI})$ ($10^8 M_{\odot}$)	$0.77^{(2)}$	$2.36^{(2)}$
M_{dyn} ($10^8 M_{\odot}$)	$4^{(2)}$	$14^{(2)}$
$M(\text{HI})/L_B$ ⁽⁸⁾	$0.50^{(2)}$	$1.10^{(2)}$

(1) – from Kniazev et al. (2000)

(2) – derived in this paper; velocities are from a gaussian fit

(3) – from Pustilnik et al. (2003)

(4) – corrected for Galactic extinction $A_B = 0.20$

(5) – $a \times b$ at $\mu_B = 25^{\text{m}}0 \text{ arcsec}^{-2}$

(6) – from the optical diameters and assuming an intrinsic axis ratio of 0.2

(7) – in units of $\text{Jy} \cdot \text{km s}^{-1}$

(8) – in units of $(M/L_B)_{\odot}$

in a disk, albeit with most of the gas in an expanding ring at the periphery of the disk. While the high resolution image of HS 0822+3542 (Fig. 4) could be interpreted as emission from a ring, such an interpretation would require that the HI disk should be viewed almost perfectly edge on, i.e. the HI disk inclination must be much higher than that inferred from the optical image (see Tab.2). On the other hand, the size scale of the gas disk is much larger than that of the optical components seen in the HST image. The larger component A has an angular size of only $\sim 1.6''$; from Fig. 4[A]) this is ~ 26

times less than the deconvolved size (at a column density of $1 M_{\odot}/\text{pc}^2$) of the HI disk. The ratio of HI mass to the optical luminosity in these two components is however not so extreme, with $M(\text{HI})/(L_B^A + L_B^B) \sim 1.7$ (where we use the values for $L_B^A + L_B^B$ estimated by Corbin et al. 2005). For the system as a whole we have (from Tab. 2), $M(\text{HI})/L_B \sim 0.50$. Note that the L_B value listed in Tab. 2 has (as is generally the case for BCGs) a substantial contribution from nebular emission (including line emission) while the blue luminosities given by Corbin et al. (2005) for the two components are corrected for the contribution from strong lines.

SAO 0822+3545 has a radial velocity difference of only $\sim 16 \text{ km s}^{-1}$ and a projected separation of only $\sim 11 \text{ kpc}$ from HS 0822+3542. The characteristic dynamical time for this pair $\tau_{\text{dyn}} \sim r_p/\Delta V \sim 700 \text{ Myr}$, comparable to the rotation periods of the galaxies in the pair. It would hence seem unreasonable to treat HS 0822+3542 as an isolated system. The peculiar morphology of HS 0822+3542, with its large scale HI tails and the offset between the optical and HI emission could be due to interaction with SAO 0822+3545. The HI morphology of SAO 0822+3545, as seen on the high-resolution map in Fig. 4[D], is also very irregular, with a tail like feature to the north of the main body and an HI ‘hole’ the SE part of the optical body.

In view of the strong possibility of an external tidal trigger to the star formation in HS 0822+3542, it is worth taking a relook the scenario (earlier suggested by Pustilnik et al. 2003) where components “A” and “B” are star forming regions in a tidally disturbed galaxy. In this scenario, the “ocular” appearance of component “A” could be the result of triggered star formation (Elmegreen & Lada (1977); Elmegreen et al. 2002), where feedback from an older central star cluster has resulted in star formation in a surrounding ring. In this context, it is interesting to note that Pustilnik et al. (2003) found evidence for an expanding superbubble in HS 0822+3542. Our HI data have too low a signal-to-noise ratio to search for corresponding signatures in the HI maps. However, we note that at in the highest resolution image (Fig. 4[C]) the HI column density peaks on either side of the optical emission. Triggered star forming rings around an existing star cluster have been observed both in our own galaxy (Deharveng et al. (2003), Deharveng et al. 2005) as well as in external dwarf galaxies (Sextans A; van Dyk et al. 1998). Further, the evidence presented by Pustilnik et al. (2003) for recent star formation elsewhere in HS 0822+3542 (e.g. the arc at the northwestern edge (or the tip of the “tidal plume” in the terminology of Corbin et al. 2005)) is also probably easier to understand in this scenario than in one where HS 0822+3542 is an ongoing merger of two ultra-compact dwarfs. Finally, we note that though Corbin et al. (2005) state that the surface brightness of components “A” and “B” are a factor of ~ 100 higher than that of the stellar “tidal” plume, the values for the surface brightness given in their paper ($23 \text{ mag arcsec}^{-2}$ for the plume and $20.6 \text{ mag arcsec}^{-2}$ for component “B” and the ring in component “A”) imply that the difference in surface brightness is only ~ 9 . There hence appear to be good reasons for regarding the optical knots in HS 0822+3542 as star forming regions in a single galaxy, as opposed to merging ultra-compact dwarfs. Higher quality data and detailed numerical modelling would however be required to conclusively distinguish between these two models.

As noted by Pustilnik et al. (2003), the LSB galaxy SAO 0822+3545 is unusually blue. Further, despite a small downward correction of its H_I flux relative to that given in Pustilnik et al. (2003) SAO 0822+3545 remains one of the most gas-rich known LSB galaxies, with the gas-mass fraction $M_{\text{gas}}/(M_{\text{gas}}+M_{\text{star}})$ in the range of 0.77 to 0.88, depending on the age/mass of the old stellar population. Comparison of several evolutionary models for SAO 0822+3545 with the constraints provided by its integrated colours, EW(H α), M_{gas} and M_{dyn} favours the scenario where the optical emission comes from a mixture of a young stellar population ($t_1 = 10$ Myr, $M_{\text{young}} = (2.4\text{--}4.4) \times 10^5 M_{\odot}$) and an ‘old’ stellar population (with age in the range of 0.25 to 10 Gyr and mass M_{old} of 10–30 M_{young}). Such a ‘starburst’ event with the instantaneous formation of $\sim 3 \times 10^5 M_{\odot}$ and a release of a large amount of kinetic energy in the form of stellar winds and SNR should have a measurable effect on the neutral gas; in particular one might expect to see H_I ‘holes’. Indeed, in Fig. 4[D] we see that in the optically brighter south-east edge there is a clear deficit of H_I gas. We note however that this deficit is seen mainly in the high resolution image, and that it is possible that the ‘hole’ is filled with low column density gas. If we do treat the feature as a ‘hole’, it corresponds to a linear size of ~ 500 pc. McCray & Kafatos (1987) give a relation between the hole size R and the number of supernovae (N_*) producing the hole, viz.

$$R \sim 97(N_*E_{51}/n_0)^{1/5}t_7^{3/5}$$

where E_{51} is the energy per supernovae in units of 10^{51} erg, n_0 is the ambient density in atoms cm^{-3} and t_7 is the age in units of 10^7 yr. If we take E_{51} , n_0 and t_7 to be ~ 1 , we find that the energy output from ~ 5 supernovae would be sufficient to produce a hole this size. This number of supernovae is easily produced by a young stellar population with mass $\sim 2 \times 10^5 M_{\odot}$ (from e.g. PEGASE2; Fioc & Rocca-Volmerange 1999). While detailed modelling and better H_I and optical data would be essential to see if the H_I ‘hole’ that we see has been produced by feed back from the star burst, the above calculation does indicate that a young stellar population with mass similar to that inferred by Pustilnik et al. (2003) should in principle be able to produce a hole comparable in size to the galaxy itself.

Finally we note that the peak inclination corrected H_I column densities in HS 0822+3542 are comparable to the observed threshold for star formation in dwarf galaxies ($N_{\text{HI}} \sim \times 10^{21}$ atoms cm^{-2} ; Skillman 1987). While star formation is indeed ongoing in HS 0822+3542, the peak H_I column density is offset from the sites of current star formation (4[C]). This may be a consequence of feedback (either in the form of ionization or evacuation). Similarly, the H_I column density in SAO 0822+3545 (see Fig. 4[D]) is above the threshold value over a large fraction of its area. In particular, the prominent double H_I blob on the east edge of the galaxy has high density, but no traces of star formation. There are several other known cases of dwarf galaxies where current star formation is offset from the location of the peak H_I column density (e.g. SBS 0335–052; Pustilnik et al. 2001), and, in a detailed study of the relation between star formation and H_I column density in a sample of nearby extremely faint dwarf galaxies Begum et al. (2006) found no

one to one correspondence between high H_I column density and ongoing star formation.

In summary, our GMRT observation of the galaxy pair HS 0822+3542/SAO 0822+3545 shows (i) some evidence for tidal interaction, (ii) that the H_I emission from HS 0822+3542 has an angular size ~ 25 times larger than that of the optical components identified in the HST imaging, and (iii) that the H_I properties of the galaxies are in general similar to those of comparably sized gas rich dwarf galaxies. We suggest that the optical knots in HS 0822+3542 are star forming regions in a tidally disturbed dwarf galaxy as opposed to being merging ultra-compact dwarfs.

Acknowledgements The observations presented in this paper were obtained using the GMRT which is operated by the National Centre for Radio Astrophysics (NCRA) of the Tata Institute of Fundamental Research (TIFR), India. SAP acknowledges partial support from the Russian state program “Astronomy” and from the RFBR grant No.06-02-16617. This research has made use of the NASA/IPAC Extragalactic Database (NED), which is operated by the Jet Propulsion Laboratory, California Institute of Technology, under contract with the National Aeronautics and Space Administration. The authors acknowledge the SDSS database for the images used for this study. Funding for the Sloan Digital Sky Survey (SDSS) has been provided by the Alfred P. Sloan Foundation, the Participating Institutions, the National Aeronautics and Space Administration, the National Science Foundation, the U.S. Department of Energy, the Japanese Monbukagakusho, and the Max Planck Society. The SDSS Web site is <http://www.sdss.org/>. The SDSS is managed by the Astrophysical Research Consortium (ARC) for the Participating Institutions. The Participating Institutions are The University of Chicago, Fermilab, the Institute for Advanced Study, the Japan Participation Group, The Johns Hopkins University, the Korean Scientist Group, Los Alamos National Laboratory, the Max-Planck-Institute for Astronomy (MPIA), the Max-Planck-Institute for Astrophysics (MPA), New Mexico State University, University of Pittsburgh, University of Portsmouth, Princeton University, the United States Naval Observatory, and the University of Washington. We thank the referee for comments that resulted in a substantial improvement in the quality of this paper.

REFERENCES

- Abazajian K., et al., 2005, AJ, 129, 1755
- Begum A., Chengalur J. N., 2004, A&A, 413, 525
- Begum A., Chengalur J. N., Hopp U., 2003, New Astronomy, 8, 267
- Begum A., Chengalur J. N., Karachentsev I. D., Kaisin S. S., Sharina M. E., 2006, MNRAS, 365, 1220
- Corbin M. R., Vacca W. D., Hibbard J. E., Somerville R. S., Windhorst R. A., 2005, ApJL, 629, L89
- Deharveng L., Lefloch B., Zavagno A., Caplan J., Whitworth A. P., Nadeau D., Martín S., 2003, A&A, 408, L25
- Deharveng L., Zavagno A., Caplan J., 2005, A&A, 433, 565
- Ekta, Chengalur J. N., Pustilnik S. A., 2006, MNRAS (in press), (Paper II)
- Elmegreen B. G., Lada C. J., 1977, ApJ, 214, 725

Elmegreen B. G., Palouš J., Ehlerová S., 2002, MNRAS, 334, 693

Fioc M., Rocca-Volmerange B., 1999, astro-ph/9912179

Higdon J. L., 1996, ApJ, 467, 241

Kniazev A. Y., et al., 2000, A&A, 357, 101

Koribalski B., Gordon S., Jones K., 2003, MNRAS, 339, 1203

Kregel M., Sancisi R., 2001, A&A, 376, 59

Kunth D., Östlin G., 2000, ARAA, 10, 1

McCray R., Kafatos M., 1987, ApJ, 317, 190

Pettini M., Smith L. J., King D. L., Hunstead R. W., 1997, ApJ, 486, 665

Pustilnik S. A., Brinks E., Thuan T. X., Lipovetsky V. A., Izotov Y. I., 2001, AJ, 121, 1413

Pustilnik S. A., Kniazev A. Y., Pramskij A. G., Uglyumov A. V., Masegosa J., 2003, A&A, 409, 917

Pustilnik S. A., Pramskij A. G., Kniazev A. Y., 2004, A&A, 425, 51

Pustilnik S. A., et al., 2005, A&A, 442, 109

Pustilnik S. A., Martin J.-M. 2006, A&A (submitted), (Paper I)

Skillman E. D., 1987, in Star Formation in Galaxies pp 263–266

Springel V., Hernquist L., 2005, ApJL, 622, L9

Staveley-Smith L., Davies R. D., Kinman T. D., 1992, MNRAS, 258, 334

Swarup G., Ananthakrishnan S., Kapahi V. K., Rao A. P., Subrahmanya C. R., Kulkarni V. K., 1991, Cur. Sci., 60, 95

Thuan T. X., Lipovetsky V. A., Martin J.-M., Pustilnik S. A., 1999, A&AS, 139, 1

van Dyk S. D., Puche D., Wong T., 1998, AJ, 116, 2341